Advance Publication by J-STAGE

Electrochemistry

The Electrochemical Society of Japan

Received: April 23, 2019
Accepted: August 23, 2019
Published online: November 11, 2019

https://doi.org/10.5796/electrochemistry.19-00033

Article

Electrochemistry, (in press)

Enhanced Li Ion Storage Performances of Carbon Black by Introducing Organosulfur Groups on Surface

Kun WANG,[b] Dongying JU,[b,c] Guiying XU,[a] Beibei HAN,[c] Yongfei WANG,[a] Jian ZHANG,[a] Maorong CHAI,[c] Shaobei CHEN,[a] and Weimin ZHOU[a,*]

[a] *Institute of Energy Materials and Electrochemistry, School of Chemical Engineering, University of Science and Technology Liaoning, Anshan 114051, P. R. China*
[b] *School of Materials and Metallurgy, University of Science and Technology Liaoning, Anshan 114051, P. R. China*
[c] *Advanced Science Research Laboratory, Saitama Institute of Technology, 1690 Fusaiji, Fukaya, Japan*

* *Corresponding author: aszhou15242870697@163.com*

ABSTRACT

The carbon black (CB) is modified successfully by the two-step modifications such as organo-chlorination and organo-sulfuration using the chemical reagents of thionyl chloride and ethanethiol continuously. The organosulfur groups of –C–SR and –COSR forming on the CB surface play the main role to improve the electrochemical performances, which is verified by electrochemical studies. For instance, after carrying out the charge-discharge 100 times, the organosulfur modified CB (MCB) shows the Li^+ ion storage capacity at 392 mAh/g, which is higher than CB showing at 176 mAh/g. Furthermore, the improvement storage capacity is attributed to the enhanced capacitive effects which are verified by the detailed measurements of cyclic voltammetry (CV). These results are able to provide effective way to enhance the storage capacity of general carbon materials such as CB, graphite, graphene oxide (GO) and so on.

Keywords : Modified Carbon Black (MCB), Organosulfur Modification, Li^+ Ion Batteries (LIBs), Organic-inorganic Hybrid

1. Introduction

Nowadays, the LIBs have been attracted than ever before, for they can be applied in various fields such as electrical appliances and electric vehicle (EV).[1–5] In particular, countries all over the world are paying noticeable attention to the popularity of EV, in attempt to achieve a low carbon emission society. The energy density and cost of LIBs are, however, becoming the technical hurdle gradually, which constrains their applications on the EV. Therefore, how to increase the energy density and decrease the fabrication cost of LIBs is becoming the besetting problem for great many of researchers.

To increase the Li^+ ion storage capacity of carbon materials, the hybrid concept is widely used. For example, some hybrid materials were fabricated by carbon with Si, Ge and Sn elements, respectively.[6–8] Although, the storage capacity of these hybrid materials is improved remarkably, the relatively high cost constricts their actual application as electrode materials of LIBs. As a consequence, developing the new methods to improve the storage capacity of general carbon materials with low cost is becoming a critical subject gradually.

We attempt to use the hybrid concept to improve the Li^+ ion storage capacity of general carbon materials. Especially, the CB is widely used as electrode materials because it has the excellent conductive properties as inexpensive industrial raw materials. In general, the modification method is a popular way to give CB the high value-added.[9–11] Similarly, in our previous studies, we successfully introduced the organosilicon groups such as –OSiR and –COOSiR groups on the surface of CB.[12] In this previous report, with giving the Li^+ storage capacity to the organosilicon modified CB (MCB), the itself inherent conductivity is not lost, which leads us to consider the organic-inorganic hybrid concept is the one of effective ways to enhance the Li^+ ion storage capacity of CB.

In addition, to increase the Li^+ ion storage capacity and the electrochemical stability of CB further, in this study, we also aim at the same way to introduce the organosulfur groups on CB surface, and successfully introduced the –SR and –COSR on the surface of CB. The organosulfur MCB shows the excellent Li^+ ion storage capacity at 671 mAh/g on the first cycle, and 392 mAh/g after cycling the charge-discharg 100 times, which is higher than that of organosilicon MCB.[12] However, in Li^+ ion storage mechanism, differing from the general Li/S batteries,[13–15] the capacitive effects contributed to the noticeable improvement of storage capacity of organosulfur MCB, which was determined by detailed measurements of FT-IR and CV. These results expand the usage of CB in application as anode electrode of LIBs not only, but also give the simple and effective way to improve the electrochemical performances of general carbon materials.

2. Experimental

2.1 Materials

Carbon black (CB) N330 was purchased from OUJIN Co., Ltd., China. Thionyl chloride, anhydrous CH_2Cl_2, and triethylamine were purchased from Sinopharm Chemical Reagent Limited Corporation. Ethanethiol was purchased from Aladdin Industrial Corporation. The electrolyte of 1 M $LiPF_6$ which was obtained by adding the $LiPF_6$ into the mixture which was fabricated by the ethylene carbonate/ethyl methyl carbonate/dimethyl carbonate (1:1:1, vol%). The electrolyte was purchased from Bejing Institute of Chemical Reagents.

2.2 Characterization

The FT-IR results were determined by the instrument of Nicolet Company, USA. The measurements of X-ray diffraction (XRD) were performed by the X'pert Powder instrument from PANalytical, Holland. The X-ray photoelectron spectroscopy (XPS) measurement was carried out by Quantum 2000 of ϕ Physical Electronics, USA. Electrochemical Workstation CHI660E (CHI instruments, China)

was used to carry out electrochemical experiments. The evaluations regarding the charge and discharge performances were carried out by the LAND battery test system (LAND CT2001A, China). The scanning electron microscope (SEM) morphologies of materials were evaluated by instrument (SIGMA 500) of Carl Zeiss AG, Germany. The Brunauer-Emmett-Teller (BET) measurements were carried out by Autosorb-iQ, USA. The slurry containing active materials were coated on the Cu foil by adjustable film applicator purchased from Pusheng Testing Instrument (Shanghai) Co., Ltd.

2.3 Organo-sulfur modification of CB

Carbon black N330 (15 g) was added respectively into the two conical flasks (500 mL) containing the anhydrous dichloromethane (CH_2Cl_2) solvent (200 mL). Then the two conical flasks containing the mixture of CB and CH_2Cl_2 were placed into the ice-water bath, the thionyl chloride (0.33 mL) was added and the obtained mixture was stirred for 2 hours under reflux at 45°C. The reacted mixture was filtered, and the obtained MCB was washed by anhydrous dichloromethane (CH_2Cl_2) many times. After adding the MCB into the two conical flasks (500 mL), the anhydrous CH_2Cl_2 (200 mL) was added immediately. At the same time, the ethanethiol (0.43 mL) and triethylamine (0.60 mL) were added into the same flasks quickly, and the obtained mixture was stirred for 5 hours under reflux at 45°C. The same modified reaction was also conducted using the ethanethiol (1.43 mL) and triethylamine (0.60 mL). Finally, the reacted mixtures were filtered and washed continuously by solvents of CH_2Cl_2 and water. The obtained solids were dried by vacuum for 12 h at 60°C, in order to remove the remained solvents on surface of organosulfur MCB.

2.4 Electrochemical experiments

To prepare the electrodes used for the electrochemical measurements, the organosulfur MCB (0.08 g) was mixed with acetylene black (0.01 g) and polyvinylidine fluoride (PVDF) binder (0.01 g) in a weight ratio of 80:10:10 in N-methyl-2-pyrrolidone (NMP) to ensure the homogeneity, respectively. The obtained slurry was coated on Cu foil and dried in vacuum drying oven at 80°C for 1 h to remove solution. Subsequently, the Cu foil with the active materials were dried at 120°C for 12 h in the same vacuum drying oven and cut into round shape strips of φ 11 mm in size. The two-electrode electrochemical cells were assembled in a glove box filled with high-purity argon, where the lithium metal foil (φ 15.60 mm × 0.45 mm) was used as cathode, fiberglass as separator, and 12–13 wt% of $LiPF_6$ in the mixture of EC, DMC, EMC was used as electrolyte. Charge-discharge test was carried out by LAND battery test system. The same electrochemical cells were also used to carry out measurements of CV.

3. Results and Discussion

In order to explore the possibility of organosulfur MCB in actual applications, the amount of CB was expanded to 15 g, compared with our previous report.[12] As shown in Scheme 1, we carried out the organo-chlorination of CB by reaction of CB with thionyl chloride firstly. After C-Cl groups were introduced on the CB surface, the next modified reaction of CB-Cl with ethanethiol proceeded continuously. Referring to our previous report (total number of moles of –COOH and –OH of CB are 2.54×10^{-4} mol/g),[12] the amount of thionyl chloride showing at 3.05×10^{-4} mol/g was used firstly. Secondly, the amounts of ethanethiol showing at 3.81×10^{-4} mol/g and 1.27×10^{-3} mol/g were used respectively. Namely, the number of moles of thionyl chloride and ethanethiol were against the total number of moles of –OH and –COOH groups on CB surface at 1.2 and 1.5, 5.0 times, respectively. To easily describe as follows, the organosulfur MCB (obtained by the modified reactions using the CB with ethanethiol having the mole number as 1.5 times and 5 times against the total mole numbers of –OH and –COOH groups on the CB surface) were named as MCB(α) and MCB(β), respectively.

The FT-IR was used to assign the structures of CB-SR and CB-COSR whether or not formed on the CB surface. Firstly, as shown in Fig. 1b, the special peaks of triethylamine hydrochloride did not observe completely, indicating that organosulfur MCB has high purity after washing process using the anhydrous dichloromethane solvent. Compared with the Fig. 1a, the novel characteristic peaks assigned to the MCB(β) were clearly observed in Fig. 1b. As an example, the peak of 1113 cm^{-1} indicated the –SR groups formed obviously. Meanwhile, the novel peak about 1739 cm^{-1} was

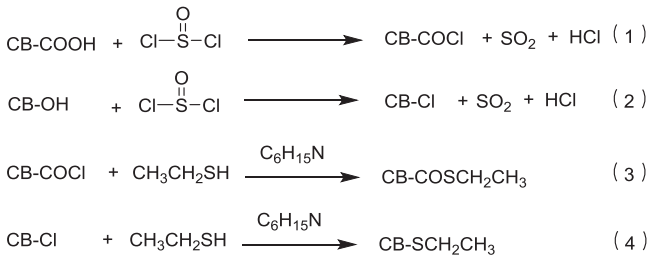

Scheme 1. The organosulfur modified process of CB.

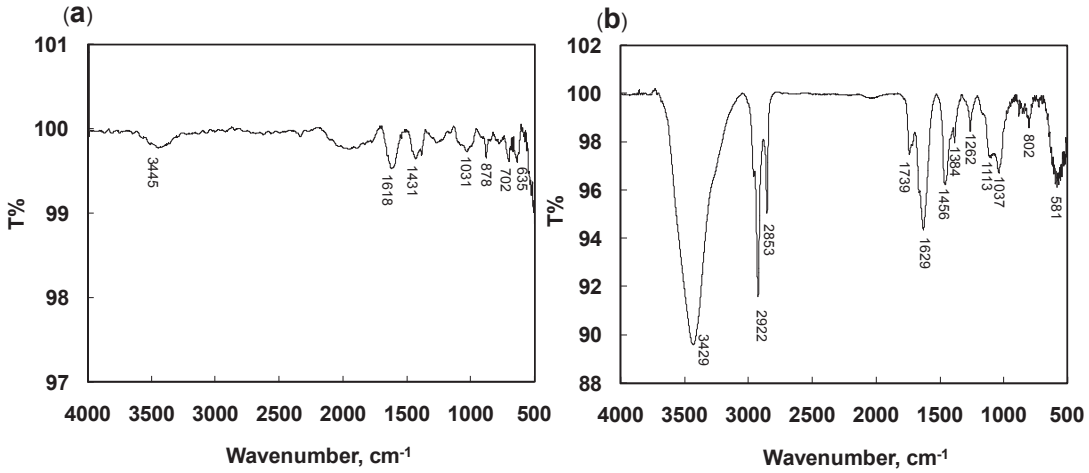

Figure 1. The FT-IR spectra of CB (a) and MCB(β) (b) which is obtained by the modification of usage of ethanethiol with 5 times against the total number of moles of –OH and –COOH groups on the CB surface.

observed evidently, which led us to consider the groups of –COSR formed on the surface of CB. Especially, the characteristic peak of alkyl groups showing at 2922 cm^{-1} was observed, indicating the –SR and –COSR groups were introduced on the surface of CB successfully.

The Raman measurements were used to verify the conversions of structures of CB, MCB(α) and MCB(β). The broad D-band peak of CB, MCB(α) and MCB(β) showed at 1359 cm^{-1}, 1356 cm^{-1} and 1362 cm^{-1}, respectively, and G-band peaks showed at 1593 cm^{-1}, 1591 cm^{-1} and 1591 cm^{-1}, respectively. Moreover, it is acknowledged that I_d/I_g values reflect the disordering of general carbon materials. To obtain the accurate I_d/I_g values, the I_d and I_g are generally used as integral areas values. Therefore, the four signals were deconvoluted in the overall Raman spectrum by Origin Software (Fig. 2).[16–19] As a result, the I_d/I_g values showed at 2.4, 2.6 and 2.8, respectively, indicating the MCB(β) possessed the more unordered structure than CB and MCB(α). These results are also indicative of the organosulfur structures were successfully introduced on the surface of CB from another perspective.

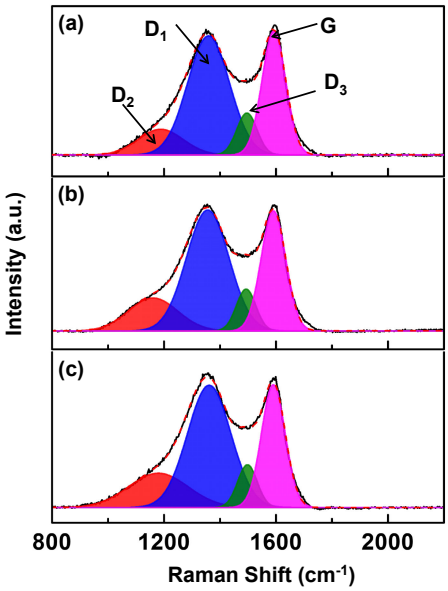

Figure 2. Raman spectra and fitting results of samples, (a) is the result of CB, (b) is the result of MCB(α) and (c) is the result of MCB(β). Thereinto, D_1 peak commonly refers to a breakdown of symmetry of carbon atoms at the edge of graphene layers, D_2 peak is assigned to carbon atoms placing on the outside of planar of graphene network, D_3 peak can be attributed to distortions of the inner symmetry in aromatic rings.

On the other hand, according to the reports of Guo et al.,[20,21] the groups on surface of CB were investigated by measurements of XPS. However, the ideal measurement results were not obtained, for the substituted S element showed the relatively lower ratio than other elements on the CB surface (Fig. S1). Meanwhile, the obvious differences in morphologies of CB, MCB(α) and MCB(β) were also not clearly observed by measurements of SEM (Fig. S2).

Moreover, the specific surface area of CB, MCB(α) and MCB(β) were evaluated by measurements of BET (Fig. 3). As a result, the specific surface area of CB, MCB(α) and MCB(β) showed at 66.5 m^2/g, 62.9 m^2/g and 62.4 m^2/g, respectively. It is obvious that introducing of organosulfur groups on CB surface slightly decreased the surface area of CB. Surprisingly, as shown in Fig. 3(b), the pore volumes of CB, MCB(α) and MCB(β) showed at 1.02 cm^3/g, 0.77 cm^3/g, and 0.75 cm^3/g, respectively. Meanwhile, it is observed that decreasing pore volumes of MCB(β) mainly occurred at pore diameter range of 22.8 nm–38.1 nm. These interest results effectively supported that organosulfur modification intensively occurred in the pore diameter range of 22.8 nm–38.1 nm of CB.

Admittedly, we could not verify how much about the modification amounts of ethanethiol was appropriate, only by the analyses of FT-IR measurements. Therefore, associating with the subsequent electrochemical evaluations, the suitable modification amounts of ethanethiol were discussed in detail.

Based on the general evaluations concerning anode materials of LIBs, we carried out the electrochemical measurements. Figure 4a(1), 4b(1) and 4c(1) illustrated the representative Li^+ ions charge-discharge curves of CB, MCB(α) and MCB(β) as anode materials at first, second, third, 50th, and 100th cycles, when the current density was adjusted to the 100 mA/g. However, the distinct plateaus were not observed clearly, similar to the most of carbon materials. Figure 4a(2), 4b(2) and 4c(2) illustrated the cycling performances of CB, MCB(α) and MCB(β). It was observed that CB, MCB(α) and MCB(β) showed the similar tendency that Li^+ ion storage capacity showed at 562 mAh/g, 692 mAh/g and 671 mAh/g on first cycle, whereas their Li^+ ion storage capacity decreased to 322 mAh/g, 422 mAh/g and 408 mAh/g, respectively when the second cycle finished. These phenomena are naturally attributed to the general explanation that solid electrolyte interface (SEI) layers formed during the first cycle. At the same time, the similar tendency was also reflected on the measurement results of coulombic efficiency. Namely, the coulombic efficiencies of Fig. 4a(2), 4b(2) and 4c(2) were at 53%, 54% and 59%, respectively, at first cycle. However, from the second cycle, they were able to be recovery

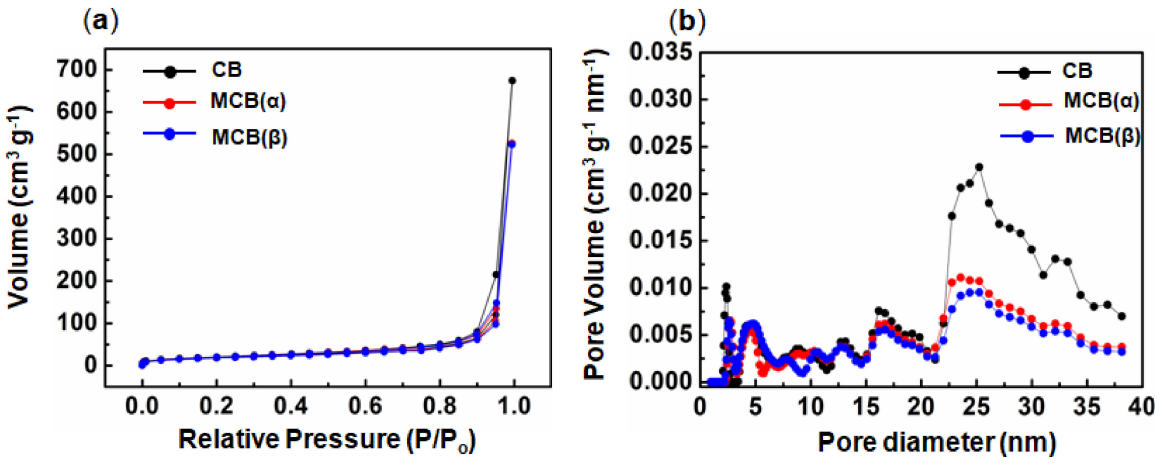

Figure 3. The results of BET are illustrated. (a) illustrates the N_2 adsorption-desorption isotherms and (b) shows the pore size distribution curves.

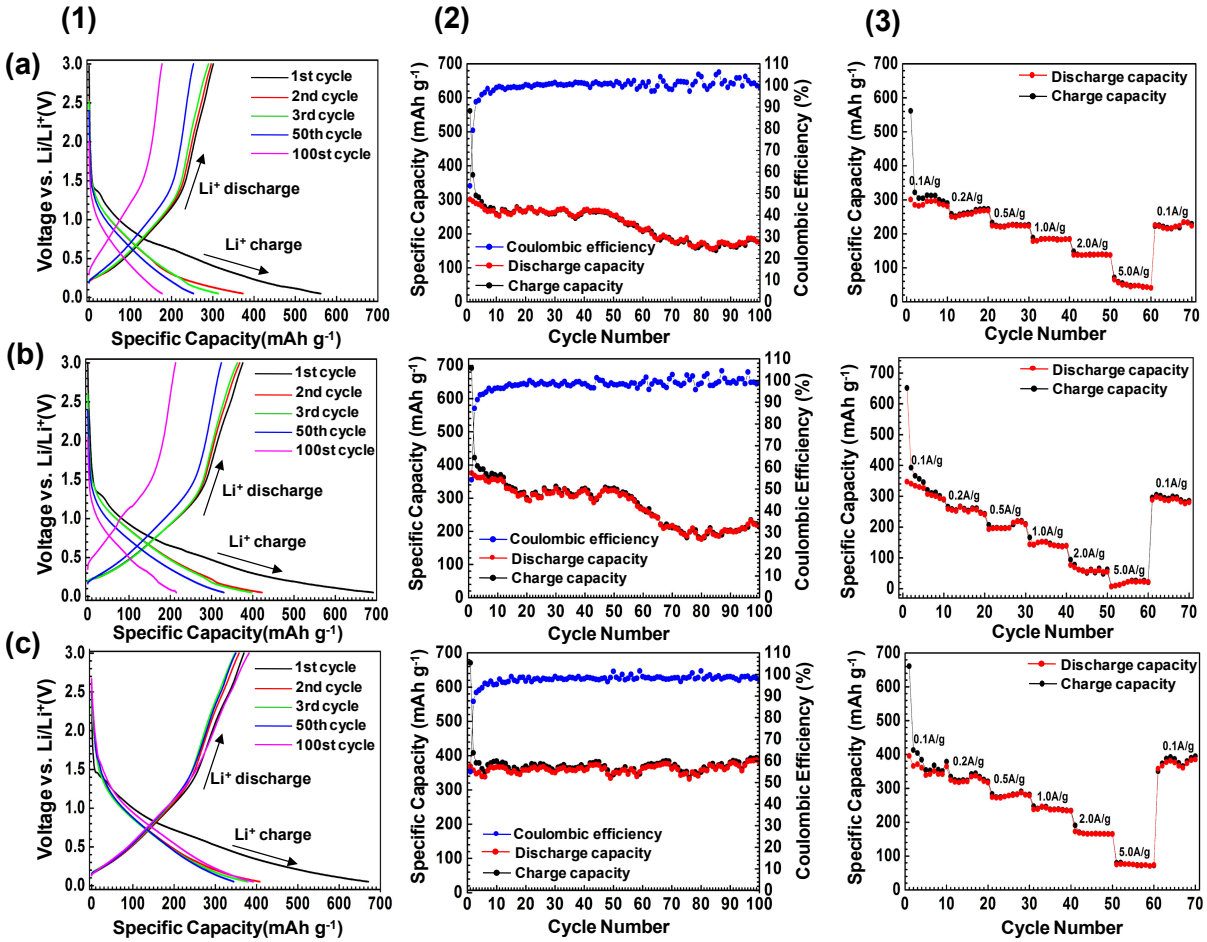

Figure 4. The electrochemical performances of CB (**a**), MCB(α) (**b**) and MCB(β) (**c**) are illustrated. (**1**) illustrates the Li^+ ion charge and discharge properties of CB, MCB(α) and MCB(β). (**2**) illustrates the cycling performances of CB, MCB(α) and MCB(β). (**3**) illustrates the rate performances of CB, MCB(α) and MCB(β).

quickly. As a result, the coulombic efficiencies maintain the high level at 99.3%, 99.2% and 97.4%, respectively, after cycling 100 times. The relatively low coulombic efficiency of MCB(β) was possibly attributed to the fact that SEI membranes probably became unstable when the introduced quantity of organosulfur group was increased.

On the other hand, compared with the Li^+ ion storage capacity such as Fig. 4a(2) showing at 176 mAh/g and Fig. 4b(2) showing at 215 mAh/g, Fig. 4c(2) possessed relative high capacity at 392 mAh/g, after being carried out the charge-discharge 100 cycles. These results about cycling performances supported that the MCB(β) possesses the higher Li^+ ion storage capacity and electrochemical performances than CB and MCB(α). Moreover, compared with the general carbon materials, the MCB(β) also shows the relatively excellent Li^+ ion storage capacity.[22,23]

According to the general evaluations about rate performances,[24,25] we carried out the charge-discharge cycles 10 times at different current densities such as 100 mA/g, 200 mA/g, 500 mA/g, 1000 mA/g, 2000 mA/g and 5000 mA/g, respectively (Fig. 4a(3), 4b(3) and 4c(3)). As a consequence, the tree cells showed the similar tendency that charge and discharge capacity decreased, with increasing the current density. It was attributed to the general reasons that polarization increases with increasing the current density.

Nevertheless, the MCB(β) showed the relatively stronger capability against the polarization than the MCB(α) and CB. As an example, when the current densities were adjusted to 100 mA/g, 500 mA/g and 5000 mA/g, respectively, the Li^+ ion storage capacity of MCB(β) showed at 661 mAh/g, 283 mAh/g and 80 mAh/g on the first cycle, which was higher than MCB(α) showing at 651 mAh/g, 196 mAh/g and 13 mAh/g, and CB showing at 562 mAh/g, 233 mAh/g and 71 mAh/g, respectively.

Furthermore, the Li^+ ion storage capacity of MCB(β) still stayed at 374 mAh/g when adjusted the current density to the 100 mA/g again, after being carried out the charge-discharge cycles 10 times at different current densities, such as 100 mA/g, 200 mA/g, 500 mA/g, 1000 mA/g, 2000 mA/g and 5000 mA/g, respectively (Fig. 4c(3)). In contrast, after carrying out the same operations with the MCB(β), the storage capacity of MCB(α) and CB only showed at 296 mA/g and 223 mAh/g which were remarkably smaller than the MCB(β) of 374 mAh/g. Consequently, we considered the MCB(β) showed the noticeable improvement capability against the polarization, compared to the MCB(α) and CB.

As shown in Fig. 5a, the oxidation potentials relating to the lithium deintercalation of MCB(α) and MCB(β) were clearly observed at 0.51 V and 0.48 V, respectively (Fig. 5a). Moreover, the MCB(β) also demonstrated the high reductive current relating to the lithium intercalation than the MCB(α) and CB in Fig. 5a. Thus, the CV measurement results also suggest that Li ion charge-discharge capacity was improved remarkably by enough introducing the organosulfur compounds on the CB surface.

On the other side, Fig. 5b manifested the electrochemical research-impedance results of CB, MCB(α) and MCB(β). As a result, the diameter of the semicircle of anode electrodes of MCB(β) was much smaller than that of CB, and MCB(α), which has been considerable that MCB(β) electrode possesses lower charge-transfer

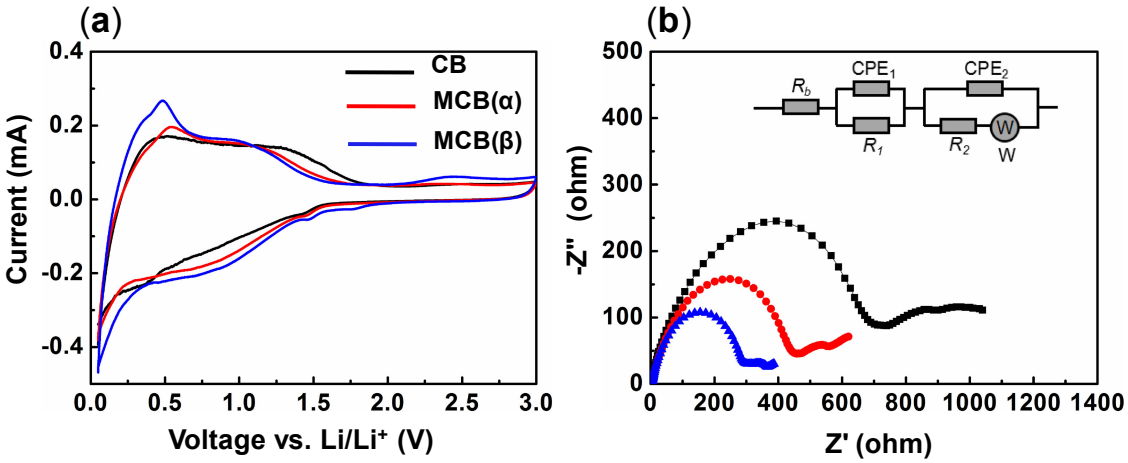

Figure 5. The CV measurement results and Nyquist plot results of CB and MCB are illustrated. (a) shows the CV curves of CB, MCB(α) and MCB(β), (b) exhibits the Nyquist plot results of CB, MCB(α) and MCB(β), which is over the frequency range of 100 kHz–0.01 Hz and amplitude of 5 mV. The R, CPE and W belong to the equivalent circuit fitting to the plots represent resistance, constant phase element and Warburg resistance, respectively.

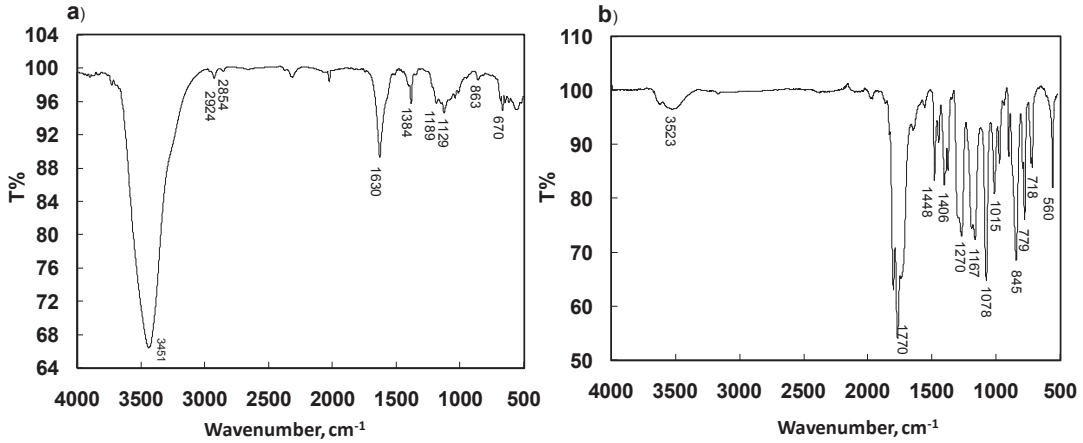

Figure 6. The FT-IR spectra are illustrated. (a) is the FT-IR spectrum of MCB(β) after being carried out charge-discharge cycling 100 times. (b) is the FT-IR spectrum of solid obtained after removing the solution of electrolyte.

impedances. In addition, according to the reports of Guo et al.,[26] the equivalent circuit fitting to the plots was also described, and the R_1 values of CB, MCB(α) and MCB(β) were calculated to the 691 Ω, 470 Ω and 310 Ω, respectively. Meanwhile, the R_2 values were calculated to the 223 Ω, 75 Ω and 45 Ω, respectively (Table S1). These results concerning resistance indicated that MCB(β) owned the more excellent electrochemical performances than the CB and MCB(α).

In order to verify that organosulfur groups has been remained or not on the CB surface after carrying out the charge-discharge 100 times, we disassembled the cell. Then the disassembled cell was washed by the $CHCl_3$ solution for 10 minutes, and it was placed in the $CHCl_3$ solution for 1 hour. The enough washed cell was placed in the vacuum drying oven to remove the $CHCl_3$ solution. The FT-IR measurement was performed to verify the conversions of the structures of MCB(β) before and after charge-discharge cycling of 100 times.

As shown in Fig. 6, the FT-IR result of solid obtained by removing the solvent of electrolyte (Fig. 6b) was exceedingly different from the Fig. 6a, which revealed that electrolyte was removed completely after washing process. Besides, compared with the Fig. 1a, the peak around 1119 cm^{-1} attributing to the –SR groups was still observed. However, the peak about 1739 cm^{-1} assigned to the –COSR groups existing in Fig. 1b has disappeared in the Fig. 6a. At the same time, compared with the peak intensity of aromatic groups at 1630 cm^{-1}, the peak intensity of 2924 cm^{-1} decreased remarkably in Fig. 6a, comparing with that in the Fig. 1b. These results probably revealed the –COSR groups on the CB surface break approximately after cycling of 100 times, which led us to consider the electrochemical stabilities of –COSR groups were lower than the –SR groups in our studies. Therefore, the remaining organosulfur groups of –SR group on the CB surface were able to provide improvement effect for Li^+ ion storage. In view of above analyses, in order to better improve the electrochemical stability of organosulfur MCB, the improvement of electrochemical stability of –COSR groups on CB surface should be considered firstly in our next research steps.

Finally, considering the interface effect, it led us naturally to consider the storage improvements by surface modifications are whether or not capacitive effects. Thus, we performed the investigations regarding capacitances of CB and organosulfur MCB, based on the reports of Dunn et al.[27,28] As shown in Fig. 7, CB mainly showed the diffusion effect even through increased the scan rate from 0.2 mV/s to 3.0 mV/s. By contrast, the capacitive effect of the MCB(α) is stronger than the diffusion effect when increasing the scan rate from 0.2 mV/s to 3.0 mV/s. Furthermore, the MCB(β) manifested the noticeable capacitive effect in the same scan rate range. Thus, these results effectively support that

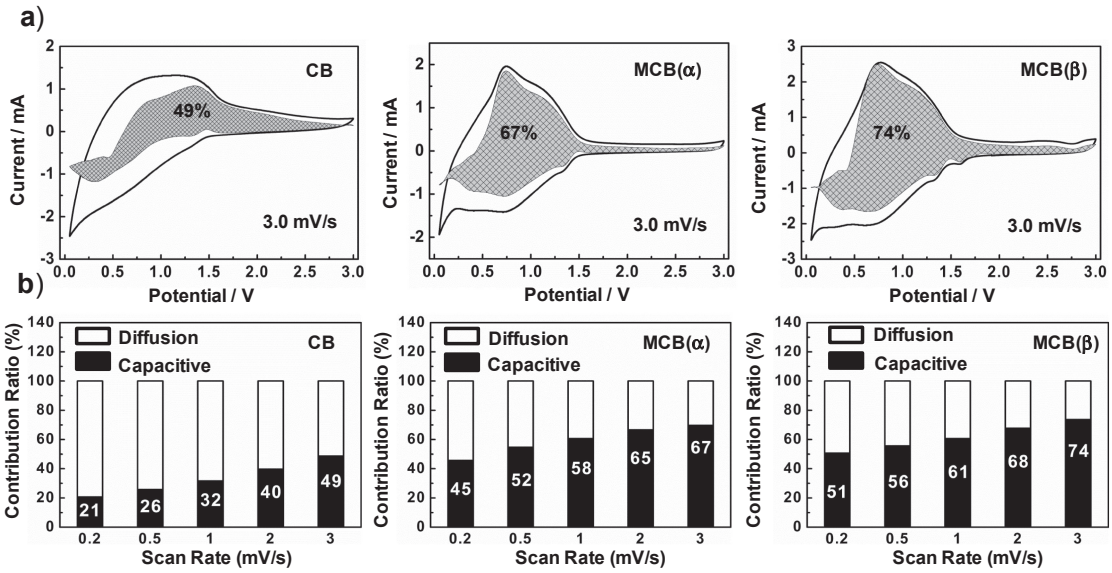

Figure 7. The capacitive contributions in storage capacity of CB, MCB(α) and MCB(β) are illustrated. Thereinto, a) is the CV curves with capacitive fraction demonstrated by the shaded area at a scan rate of 3 mV/s. b) illustrates the bar charts showing the percent of capacitive contribution at different scan rates.

introducing the organic groups on the surface of general carbon materials is able to increase their storage capacity of Li^+ ions. Finally, associating with the aforementioned BET results, we take the attitude that capacitive effects mainly appeared in the pore diameter range 22.8 nm–38.1 nm, for the organosulfur modification mainly occurred in this area (Fig. 3b).

4. Conclusions

The –SR and –OSR groups were successfully introduced on the surface of CB via the two-step modification reactions that CB reacted with thionyl chloride firstly and ethanethiol continuously. The introduced organosulfur groups on the surface of CB play the main role to improve the Li^+ ion storage capacity of organosulfur MCB. The mechanism about the improvement of Li^+ ions storage capacity is ascribed to the capacitive effects, which is verified by detailed CV measurements. Considering the fact that CB is generally used as conductive materials in fabrication of electrode materials, in our next stages, we will mix the organosulfur MCB with other general carbon materials such as graphite and graphene oxide to fabricate anodes, and their electrochemical performances will be investigated in detail. Finally, from perspective with costs being the main factor, we firmly believe that this simple improvement method can provide the useful route to widen the application of CB in the field of fabrication of anode materials for LIBs.

Supporting Information

The Supporting Information is available on the website at DOI: https://doi.org/10.5796/electrochemistry.19-00033.

Acknowledgments

We are grateful to the support of University of Science and Technology Liaoning (601009816-39) and 2017RC03. This work was partly supported by projects of the National Natural Science Foundation of China (Grant Nos. 51672117 and 51672118).

References

1. A. K. Padhi, K. S. Nanjundaswamy, and J. B. Goodenough, *J. Electrochem. Soc.*, **144**, 1188 (1997).
2. M. Armand and J. M. Tarascon, *Nature*, **451**, 652 (2008).
3. T. Tsuda, Y. Uemura, C. Y. Chen, H. Matsumoto, and S. Kuwabata, *Electrochemistry*, **86**, 72 (2018).
4. L. Li, Z. Wu, S. Yuan, and X. B. Zhang, *Energy Environ. Sci.*, **7**, 2101 (2014).
5. W. S. Jia, Q. G. Wang, J. Y. Yang, C. Fan, L. Wang, and J. Z. Li, *ACS Appl. Mater. Interfaces*, **9**, 7068 (2017).
6. M. Zhou, T. G. Cai, F. Pu, H. Chen, Z. Wang, H. Y. Zhang, and S. Y. Guan, *ACS Appl. Mater. Interfaces*, **5**, 3449 (2013).
7. Z. Q. Zhu, S. W. Wang, J. Du, Q. Jin, T. R. Zhang, F. Y. Cheng, and J. Chen, *Nano Lett.*, **14**, 153 (2014).
8. K. H. Seng, M. H. Park, Z. P. Guo, H. K. Liu, and J. P. Cho, *Nano Lett.*, **13**, 1230 (2013).
9. M. Toupin and D. Bélanger, *Langmuir*, **24**, 1910 (2008).
10. G. R. Wang, Y. S. Zhou, D. G. Evans, and Y. J. Lin, *Ind. Eng. Chem. Res.*, **51**, 14692 (2012).
11. J. Y. Wang, Y. Y. Kang, H. Yang, and W. B. Cai, *J. Phys. Chem. C*, **113**, 8366 (2009).
12. G. Y. Xu, D. L. Qu, H. F. Yu, J. Zhang, B. G. An, L. X. Li, T. J. Wang, and W. M. Zhou, *Russ. J. Appl. Chem.*, **89**, 1019 (2016).
13. Y. Yang, G. Y. Zheng, and Y. Cui, *Chem. Soc. Rev.*, **42**, 3018 (2013).
14. G. M. Zhou, D. W. Wang, F. Li, P. X. Hou, L. C. Yin, C. Liu, G. Q. Lu, I. R. Gentle, and H. M. Cheng, *Energy Environ. Sci.*, **5**, 8901 (2012).
15. D. W. Wang, G. M. Zhou, F. Li, K. H. Wu, G. Q. Lu, H. M. Cheng, and I. R. Gentle, *Phys. Chem. Chem. Phys.*, **14**, 8703 (2012).
16. Z. Liu, K. Xiao, H. Guo, X. Ning, A. Hu, Q. Tang, B. Fan, Y. Zhu, and X. Chen, *Carbon*, **117**, 163 (2017).
17. I. Herrmann, U. I. Kramm, J. Radnik, S. Fiechter, and P. Bogdanoffa, *J. Electrochem. Soc.*, **156**, B1283 (2009).
18. M. M. Shi, D. Bao, S. J. Li, B. R. Wulan, J. M. Yan, and Q. Jiang, *Adv. Energy Mater.*, **8**, 1800124 (2018).
19. X. Liu, D. Chao, D. Su, S. Liu, L. Chen, C. Chi, J. Lin, Z. X. Shen, J. Zhao, L. Mai, and Y. Li, *Nano Energy*, **37**, 108 (2017).
20. C. F. Wang, M. Zhao, J. Li, J. L. Yu, S. F. Sun, S. S. Ge, X. K. Guo, F. Xie, B. Jiang, E. K. Wujcik, Y. D. Huang, N. Wang, and Z. H. Guo, *Polymer*, **131**, 263 (2017).
21. M. J. Xu, K. Ma, D. W. Jiang, J. X. Zhang, M. Zhao, X. K. Guo, Q. Shao, E. Wujcik, B. Li, and Z. H. Guo, *Polymer*, **146**, 63 (2018).
22. X. M. Lou, C. F. Lin, Q. Luo, J. B. Zhao, B. Wang, J. B. Li, Q. Shao, X. K. Guo, N. Wang, and Z. H. Guo, *ChemElectroChem*, **4**, 3171 (2017).
23. C. F. Lin, L. Hu, C. B. Cheng, K. Sun, X. K. Guo, Q. Shao, J. B. Li, N. Wang, and Z. H. Guo, *Electrochim. Acta*, **260**, 65 (2018).
24. Y. X. Xu, Z. Y. Lin, X. Zhong, B. Papandrea, Y. Huang, and X. F. Duan, *Angew. Chem., Int. Ed.*, **54**, 5345 (2015).
25. Y. J. Zhang, J. Qu, S. M. Hao, W. Chang, Q. Y. Ji, and Z. Z. Yu, *ACS Appl. Mater. Interfaces*, **9**, 41878 (2017).
26. X. K. Cui, G. Y. Zhu, Y. F. Pan, Q. Shao, C. D. Zhao, M. Y. Dong, Y. Zhang, and Z. H. Guo, *Polymer*, **138**, 203 (2018).
27. J. Wang, J. Polleux, J. Lim, and B. Dunn, *J. Phys. Chem. C*, **111**, 14925 (2007).
28. G. Z. Fang, Z. X. Wu, J. Zhou, C. Y. Zhu, X. X. Cao, T. Q. Lin, Y. M. Chen, C. Wang, A. Q. Pan, and S. Q. Liang, *Adv. Energy Mater.*, **8**, 1703155 (2018).